Molecular Cell, Volume *40*
Supplemental Information

The miR-17-92 MicroRNA Cluster Regulates Multiple Components of the TGF-β Pathway in Neuroblastoma

Pieter Mestdagh, Anna-Karin Boström, Francis Impens, Erik Fredlund, Gert Van Peer, Pasqualino De Antonellis, Kristoffer von Stedingk, Bart Ghesquière, Stefanie Schulte, Michael Dews, Andrei Thomas-Tikhonenko, Johannes H. Schulte, Massimo Zollo, Alexander Schramm, Kris Gevaert, Håkan Axelson, Frank Speleman, Jo Vandesompele

Figure S1

(A) Relative expression of individual miR-17-92 miRNAs in MYCN amplified tumours (A), MYCN single copy high-risk tumours (SH) and MYCN single copy low risk tumours (SL) (dataset D1, supplemental table 1). Significant differential expression (Mann Whitney, $p < 0.05$) is indicated (*) (whiskers: Tukey). (B) Kaplan Meier plots for overall survival (OS) based on the pathway activity score of individual miR-17-92 miRNAs, represented as quartiles (dataset D1, supplemental table 1). Increased activity of each individual member form the miR-17-92 cluster is proportionally correlated to a poor overall survival.

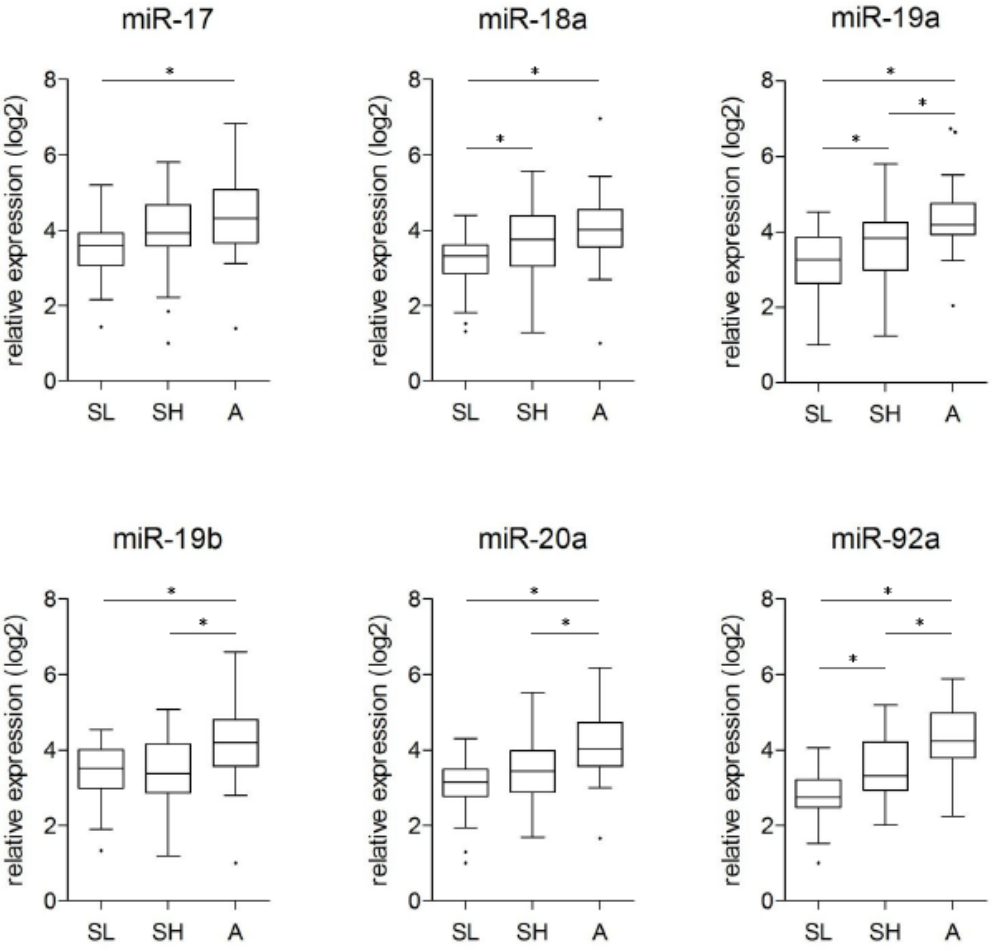
miR-17
miR-18a
miR-19a
miR-19b
miR-20a
miR-92a
relative expression (log2)
0
2
4
6
8
SL
SH
A
*

A

B

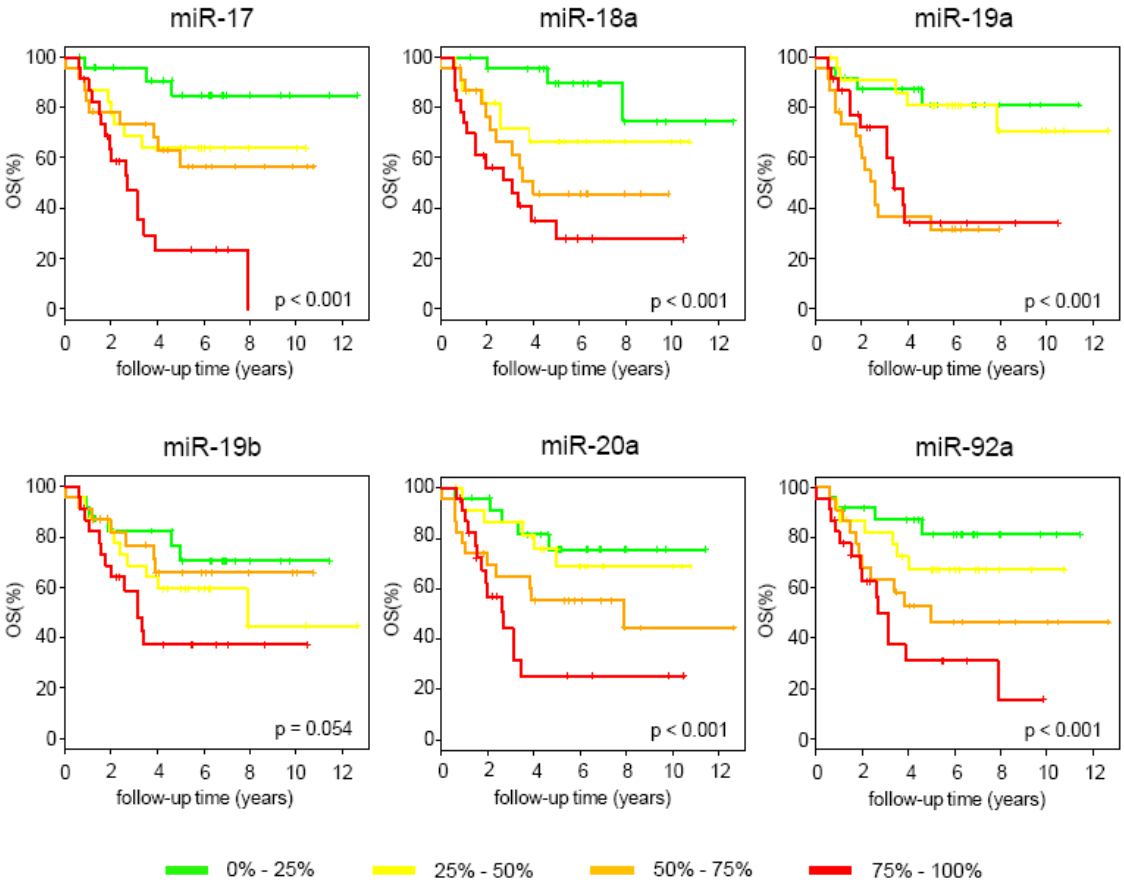
miR-17
miR-18a
miR-19a
miR-19b
miR-20a
miR-92a
OS(%)
follow-up time (years)
p < 0.001
p = 0.054
0% - 25%
25% - 50%
50% - 75%
75% - 100%

Figure S2

(A) Relative expression of miR-17-92 miRNAs upon treatment of SHEP-TR-miR-17-92 cells with tetracycline (mean ± SEM). (B) Protein quantification using LC/MS-MS. Histogram showing the number of quantified peptides per protein. (C) Histogram showing the distribution of protein fold changes of proteins that were quantified by at least 2 peptides.

A

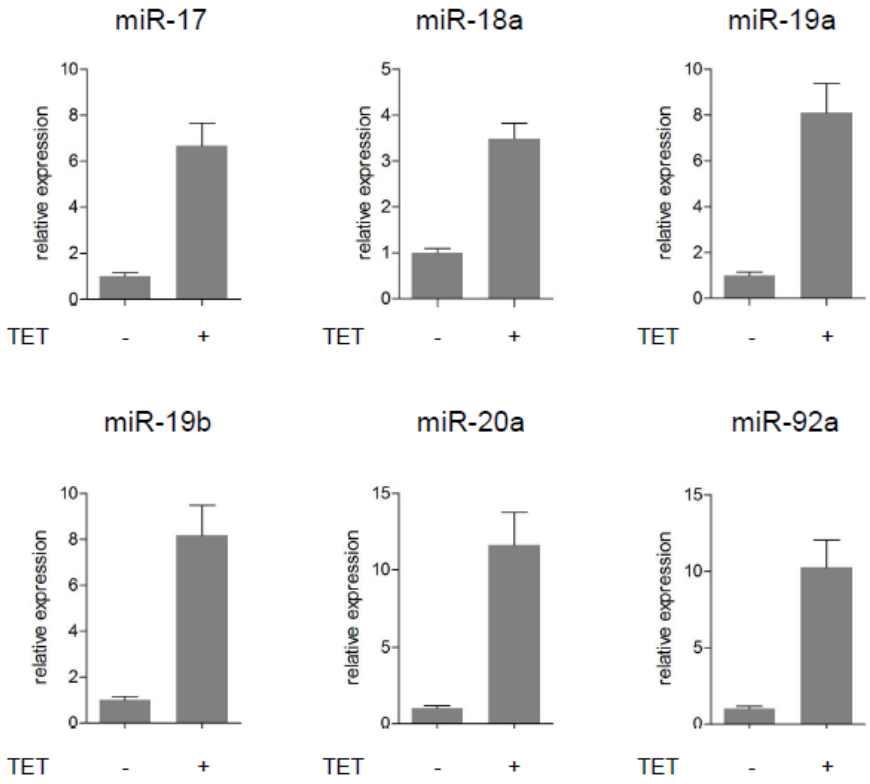

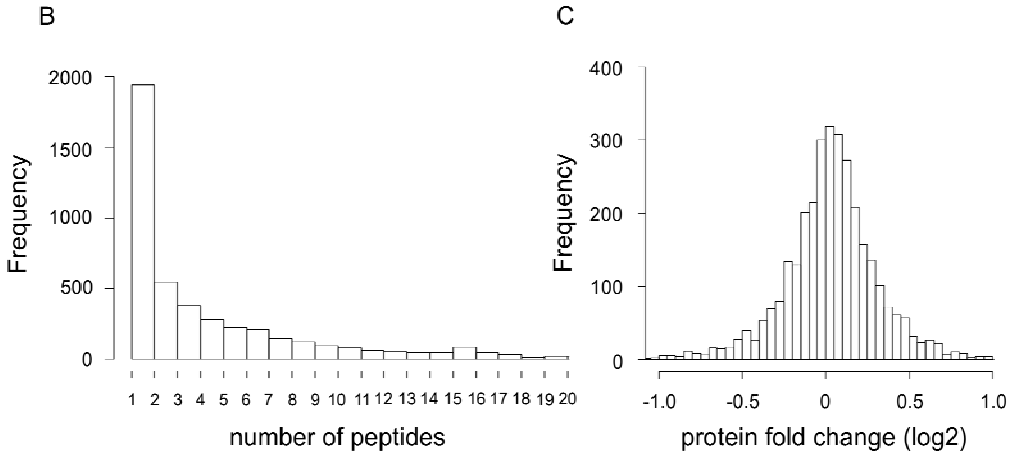

Figure S3

(A) Fraction of proteins containing at least one 7mer-8mer miR-17-92 site (black) of one 6mer-7mer-8mer miR-17-92 site (grey) in function of the protein fold change (grouped in 6 different bins according to fold change). Only downregulated proteins are shown. Dashed horizontal lines indicate the background miR-17-92 site occurrence (determined as the fraction of unchanged proteins harboring at least one 7mer-8mer miR-17-92 site of one 6mer-7mer-8mer miR-17-92 site). (B) Average number of 3'UTR miR-17-92 sites per protein in function of the protein fold change. Dashed lines indicate background measurement (calculated as in (A)). (C) Average number of miR-17-92 sites per nucleotide in function of protein fold change for 3'UTR sites (red), 5'UTR sites (blue) and coding sequence sites (CDS) (green). (D) Average fold change ± SEM of proteins for which the transcripts contain at least one 8mer miR-17-92 site in the 3'UTR (red), 5'UTR (blue) and CDS (green). (E) Number of co-occurring miR-17-92 sites in the 3'UTR of transcripts from downregulated proteins. The X-axis indicates the number of co-occurring sites between the miRNA listed on top of each graph and the miRNAs listed below each bar (miR-17/miR-20a and miR-19a/miR-19b) are analyzed together as they share identical seeds. The first bar of each graph represents the number downregulated proteins that only have one (or more) sites for the respective miRNA. Significant co-occurrence was determined by comparing results for downregulated proteins to results for a reference set (upregulated proteins) using Fisher's Exact test ($p < 0.05$).

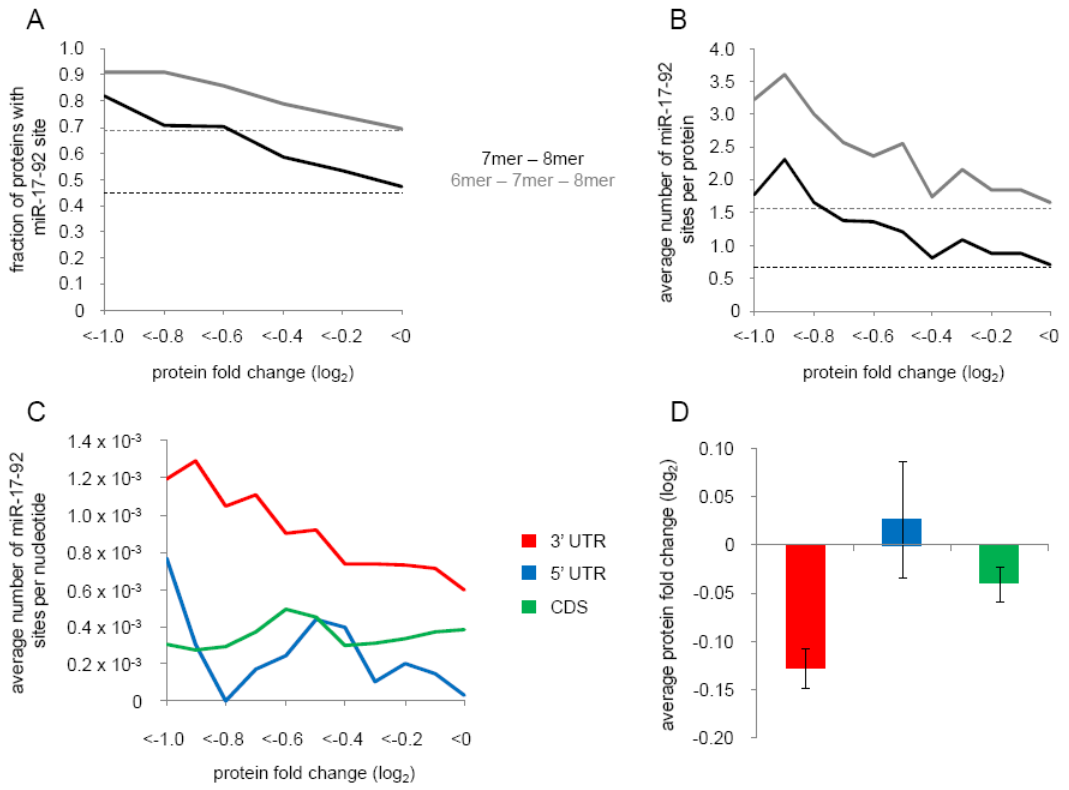

E

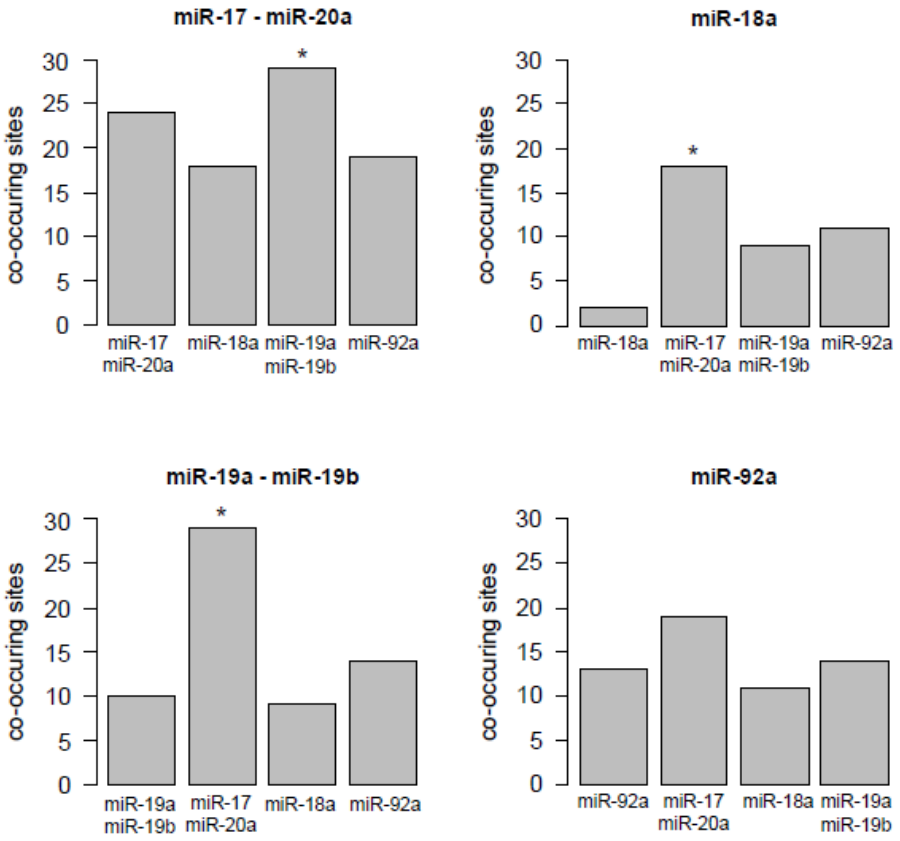
miR-17 - miR-20a
co-occuring sites
0
5
10
15
20
25
30
*
miR-17 miR-20a
miR-18a
miR-19a miR-19b
miR-92a
miR-18a
co-occuring sites
0
5
10
15
20
25
30
*
miR-18a
miR-17 miR-20a
miR-19a miR-19b
miR-92a
miR-19a - miR-19b
co-occuring sites
0
5
10
15
20
25
30
*
miR-19a miR-19b
miR-17 miR-20a
miR-18a
miR-92a
miR-92a
co-occuring sites
0
5
10
15
20
25
30
miR-92a
miR-17 miR-20a
miR-18a
miR-19a miR-19b

Figure S4

Gene set enrichment analysis plots for gene sets enriched among the proteins, upregulated upon miR-17-92 activation.

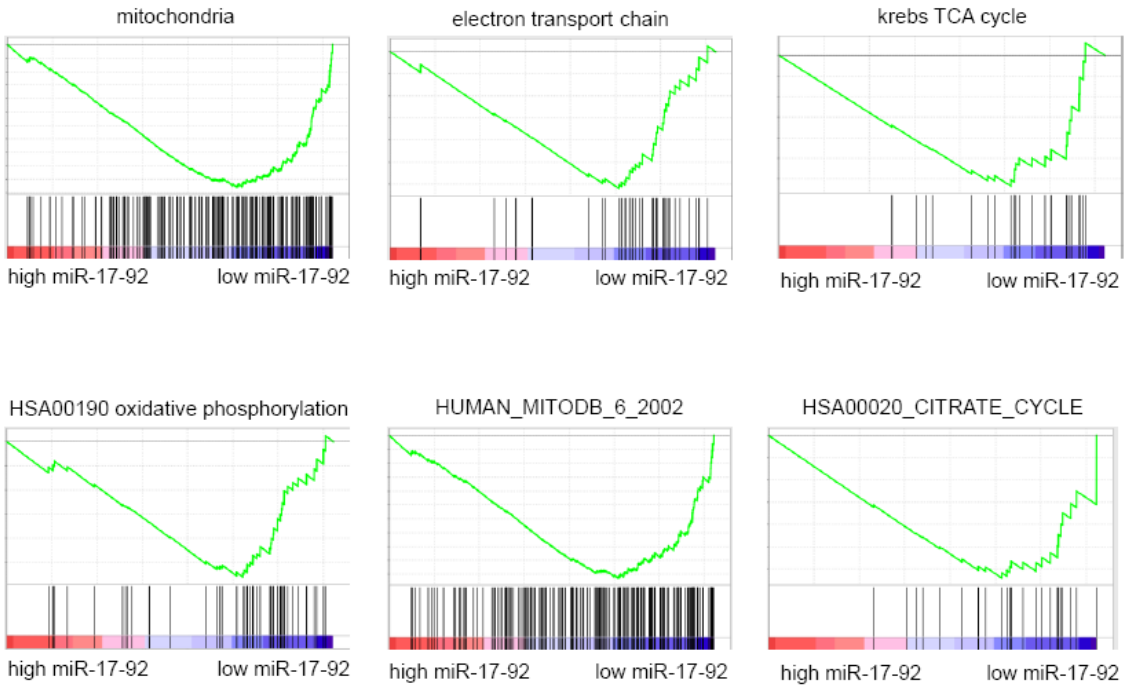

Figure S5

Relative mRNA expression (mean ± SEM) of TGFβ-responsive genes upon TET treatment of SHEP-TR-miR-17-92 cells.

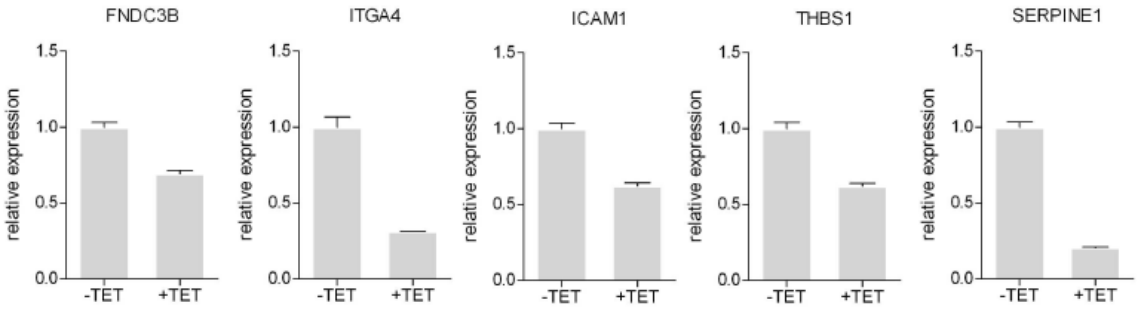

Figure S6

(A) Correlation clustering between miR-17-92 miRNA expression and TGFβ target gene expression in 40 primary neuroblastoma tumors (dataset D3, supplemental table 1). The heatmap indicates the Spearman's rank rho value. TGFβ target genes are indicated by the grey sidebar, miR-17-92 miRNAs are indicated by the black sidebar. (B) Heatmap showing relative expression of TGFβ-pathway components and target genes in neuroblastoma SHEP cells transfected with a scrambled control or with pre-miRs for the individual miR-17-92 miRNAs (miR-17, miR-18a, miR-19a, miR-19b, miR-20a and miR-92a). Black dots mark genes that have at least one 3'UTR 7mer site for the corresponding miRNA.

A

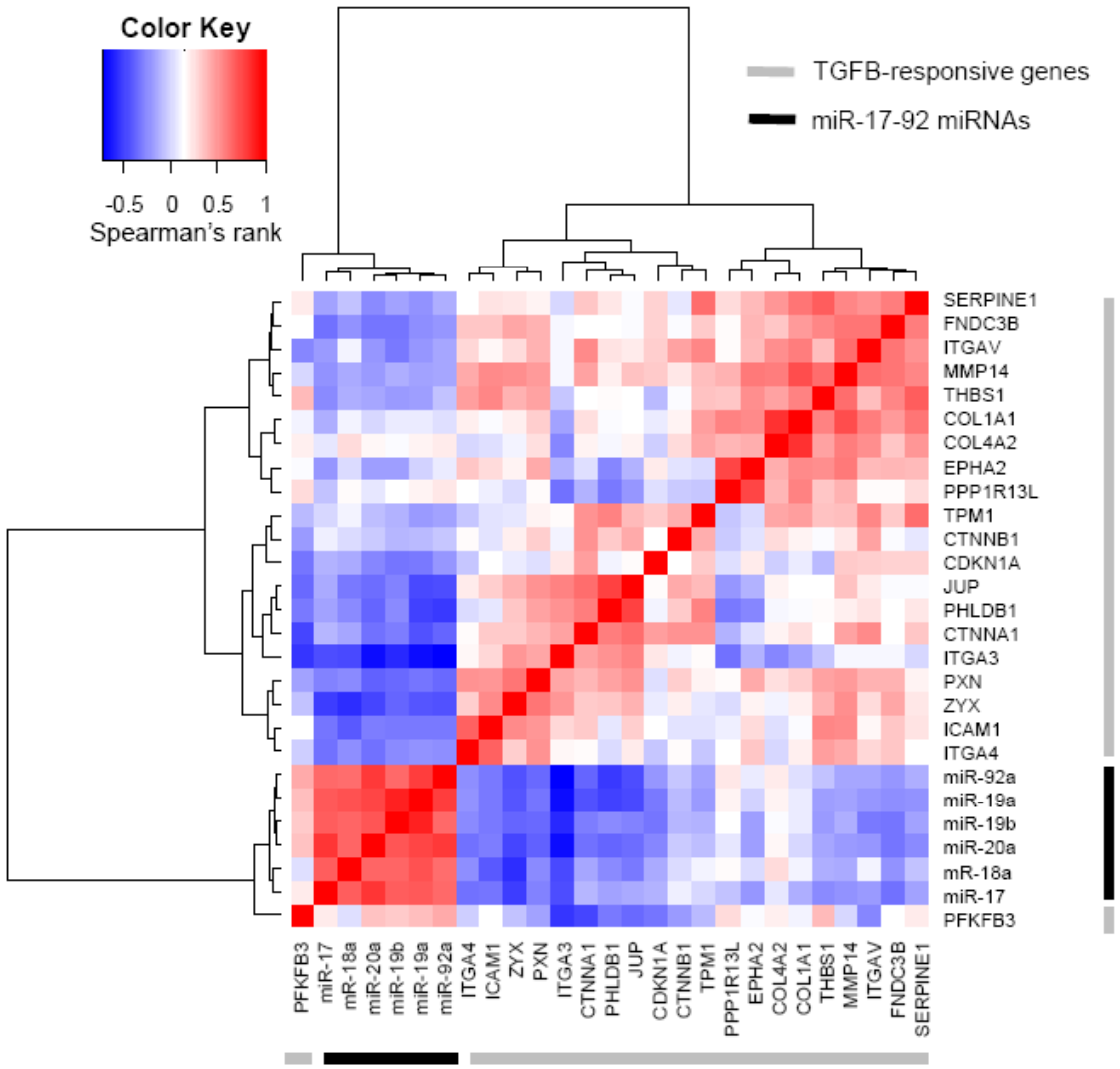

B

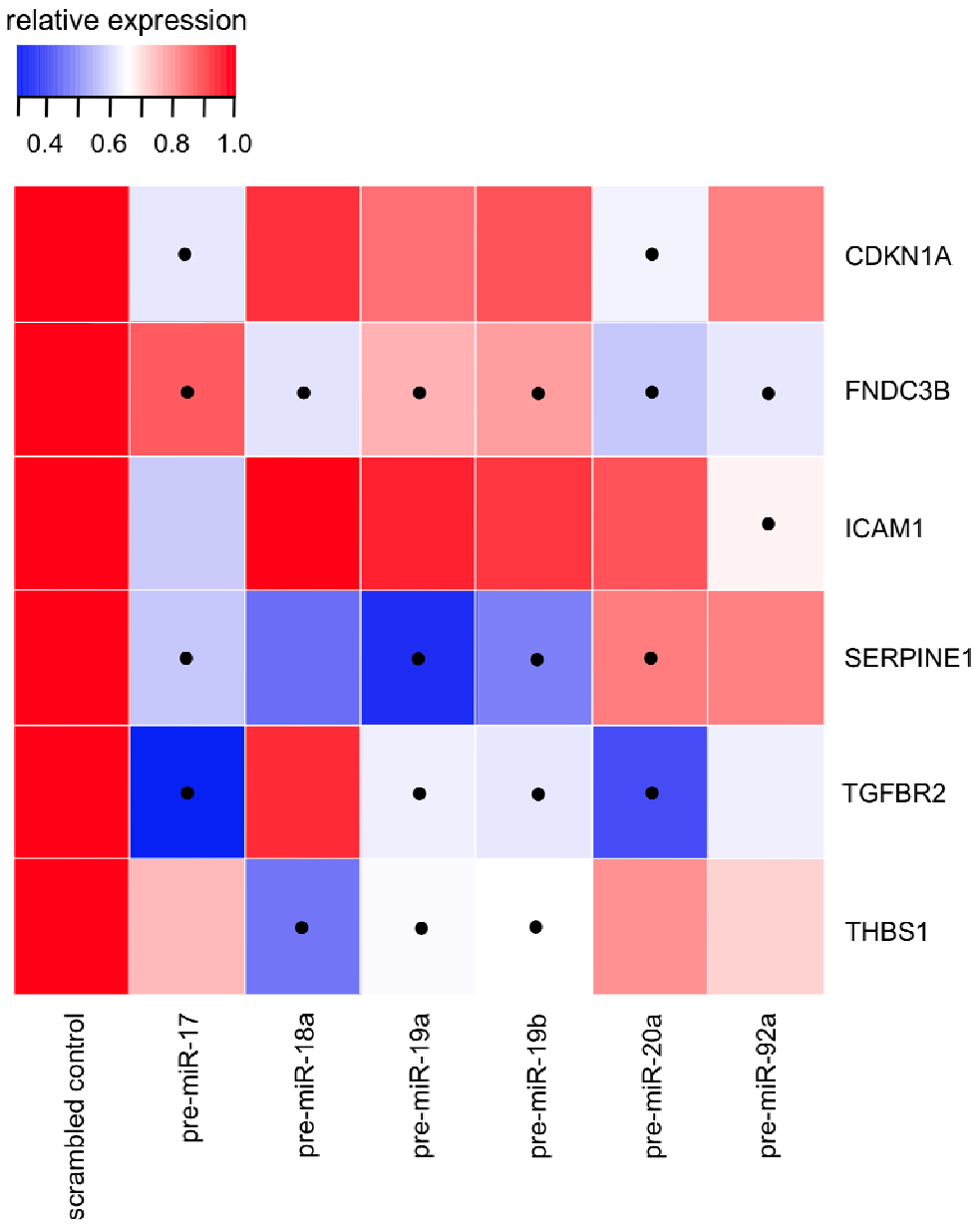
relative expression
0.4
0.6
0.8
1.0
CDKN1A
FNDC3B
ICAM1
SERPINE1
TGFBR2
THBS1
scrambled control
pre-miR-17
pre-miR-18a
pre-miR-19a
pre-miR-19b
pre-miR-20a
pre-miR-92a

Figure S7

Model for miR-17-92 mediated TGFβ pathway repression.

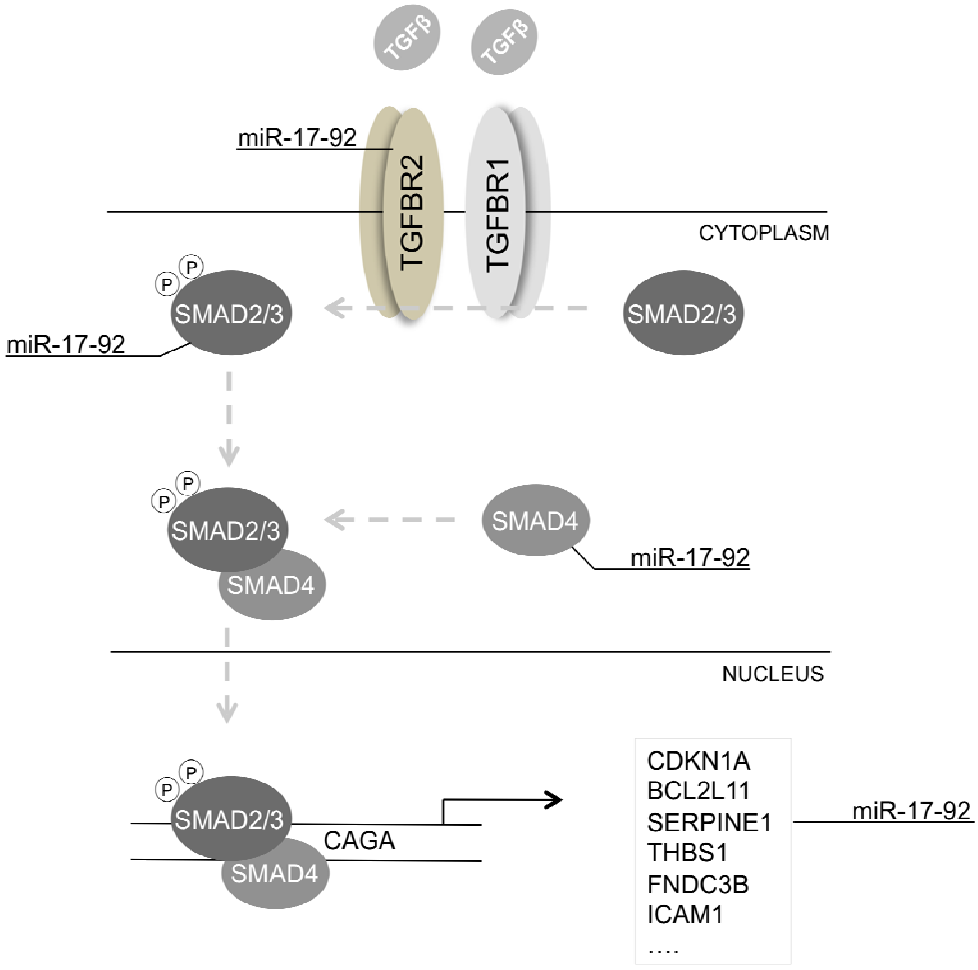

Document S2. rdml-file for RT-qPCR expression profiling of 430 miRNAs of SHEP-TR-miR-17-92 cells treated with tetracycline for 72h, provided as a separate file.

Table S1. Overview of mRNA and miRNA expression datasets

Data set ID	samples	mRNA	miRNA	reference
D1	**95**		**X**	(Mestdagh et al., 2009a)
D2	**251**	**X**		(Oberthuer et al., 2006)
D3	**40**	**X**	**X**	(Mestdagh et al., 2009a)

Table S2. Expression fold change and miR-17-92 seed frequency of all reliably measured proteins

This table is provided as a separate file.

Table S3. miR-17-92 seed occurrence and protein fold change for TGFB-target genes downregulated upon miR-17-92 activation

protein	3'UTR seed(s)	fold change (log_2)
SERPINE1	miR-17/miR-20a miR-19a/miR-19b	-1.93
THBS1	miR-18a miR-19a/miR-19b	-1.05
ITGA4	miR-17/miR-20a miR-19a/miR-19b	-0.989
FNDC3B	miR-17-92	-0.972
JUP	none	-0.869
PPP1R13L	miR-19a/miR-19b	-0.813
FILIP1L	miR-17/miR-20a	-0.735
ICAM1	miR-92a	-0.689
EPHA2	none	-0.603
COL1A1	none	-0.546
CDKN1A	miR-17/miR-20a	-0.546
PFKFB3	miR-17/miR-20a miR-19a/miR-19b	-0.544
CTNNA1	miR-18a	-0.522

Table S4. List of peptide quantifications from the forward experiment.

This table is provided as a separate file. Peptides are ordered on SwissProt accession number and increasing start position. Columns from left to right contain the SwissProt accession number, sequence of the identified peptide, start and end position of the peptide in the protein sequence, MASCOT score and threshold of the identified light (L) and/or heavy (H) component of the peptide, the L/H peptide ratio, the protein name and the L/H protein ratio.

Table S5. List of peptide quantifications from the reverse experiment.

This table is provided as a separate file. Peptides are ordered on SwissProt accession number and increasing start position. Columns from left to right contain the SwissProt accession number, sequence of the identified peptide, start and end position of the peptide in the protein sequence, MASCOT score and threshold of the identified light (L) and/or heavy (H) component of the peptide, the L/H peptide ratio, the protein name and the L/H protein ratio.

Supplemental Experimental Procedures

COFRADIC analysis

To reduce arginine to proline conversion and thus dilution of the 13C-label, the arginine concentration was lowered to 30% of its normal concentration in DMEM. Cell cultures were then treated with tetracycline for 72 hours to induce miR-17-92 expression. A biological replicate was created by swapped labeling. Cells were harvested by Versene-EDTA and washed with PBS. Cell pellets were frozen at -80ºC until further use. Prior to proteome analysis, cells were lysed in 250 µl lysis buffer containing 0.8% CHAPS in 50 mM HEPES (pH 7.4), 100 mM NaCl and 0.5 mM EDTA supplemented with protease inhibitors (Complete Protease inhibitor cocktail tablet (Roche, Basel, Switzerland); one tablet per 100 ml buffer)) for 20 minutes on ice. Cell debris was removed by centrifugation for 15 min at 16,000g at 4ºC after which the protein concentration was measured using the Biorad Protein Assay. Then, equal amounts of both proteome preparations (i.e. from differently labeled control cells or cells in which miR-17-92 expression was induced) were mixed together. To denature proteins, solid guanidinium hydrochloride was added to a final concentration of 4 M (the total sample volume was 1 ml). Proteins were then reduced and S-alkylated for 60 minutes at 30ºC by adding tris(2-carboxyethyl) phosphine and iodoacetamide to final concentrations of 3 mM and 6 mM respectively. Half of each proteome sample was then desalted on a NAP-5 column in 1 ml of 20 mM triethylamonium bicarbonate (pH 8.0). These desalted protein mixtures were heated for 5 min at 95°C, put on ice for 5 min, after which trypsin (sequencing grade, modified porcine trypsin, Promega Corporation, Madison, WI, USA) was added to a trypsin/substrate ratio of 1/50 (w/w). Trypsin digestion proceeded overnight at 37°C after which the sample was dried *in vacuo*. Dried peptides were then re-dissolved in 105 µl of solvent A (10 mM ammonium acetate (pH 5.5) in water/acetonitrile (98/2 (v/v), both Baker HPLC analysed, Mallinckrodt Baker B.V., Deventer, The Netherlands)) and 100 µl of this peptide mixture was used to isolate methionine-containing peptides by the COFRADIC technology as described previously (Gevaert et al., 2002). In this way, the complexity of the peptide mixture was reduced by a factor of about five and the hence isolated peptide mixture – which is highly enriched for methionine-containing peptides – were analyzed by LC-MS/MS using an Orbitrap XL mass spectrometer (Thermo Electron, Bremen, Germany) that was operated as previously described (Ghesquiere et al., 2009).

Generated MS/MS spectra were converted to MS/MS peak lists as described (Ghesquiere et al., 2009) and these peak lists were searched in the human fraction of the Swiss-Prot database (version 56.4, containing 20,408 human protein sequences) using a locally installed version of the MASCOT database search engine (version 2.2.04 (Perkins et al., 1999)).

Carbamidomethylation of cysteine and oxidation of methionine were set as fixed MASCOT parameters, and acetylation of a protein's N-terminus, pyro-carbamidomethyl cysteine (from N-term cysteine), pyroglutamate formation (N-term glutamine) were considered as variable modifications. Trypsin/P was set as the protease with one missed cleavage allowed and MASCOT's quantitation parameters were set to SILAC Arg and Lys + 6. Only peptide identifications that were ranked one, scored above the corresponding MASCOT threshold score for identity set at 99% confidence were considered identified. The false discovery rate of these identifications was determined according to the method described by Elias and Gygi (Elias and Gygi, 2007) and found to be 0.21% (on the spectrum level). Quantification of the identified peptides was then done using MASCOT Distiller Quantitation Toolbox (www.matrixscience .com) in the 'precursor' mode. The software tried to fit an ideal isotopic distribution on the experimental data based on the peptide average amino acid composition. This was followed by extraction of the XIC signal of both peptide components (light and heavy) from the raw data. Ratios were calculated from the area below the light and heavy isotopic envelope of the corresponding peptide (integration method 'trapezium', integration source 'survey'). To calculate this ratio value, a least squares fit to the component intensities from the different scans in the XIC peak was created. MS scans used for this ratio calculation were situated in the elution peak of the precursor determined by the Distiller software (XIC threshold 0.3, XIC smooth 1, Max XIC width 250). To validate the calculated ratio, the standard error on the least square fit had to be below 0.14 and correlation coefficient of the isotopic envelope needed to be above 0.90. The number of recorded and identified spectra as well as the number of unique peptide quantifications is indicated for both analyses in the table below. All identified spectra are made publically available in the PRIDE database (www.ebi.ac.uk/pride), accession 14860.

analysis	**# MS/MS spectra recorded**	**# MS/MS spectra identified**	**# unique peptide quantifications**
forward	83275	30141	14524
reversed	127760	32833	15875

Next, protein ratios were calculated as the average of individual peptide ratios by the in-house developed Rover algorithm (Colaert et al., 2010). Peptide ratios that could not be adequately calculated by the Distiller software were also manually validated using the Rover application (typically belonging to highly regulated peptides and proteins). Supplemental tables 4 and 5 show the Rover output and contain all peptide quantifications for the forward and reversed

experiment. In case a peptide could be derived from more than one protein sequence, all protein isoforms are listed which explains why the number of peptide quantifications in these lists exceeds the number of unique peptide quantifications in the table above. Peptide ratios of the repeated experiments were averaged and proteins that were quantified by at least 2 peptides were selected for further analysis. UniProtKB accessions were mapped to RefSeq IDs using the Biomart tool from Ensembl (www.ensembl.org).

RT-qPCR

2 µg of RNA from each sample was treated with RQ1 DNase I (Promega) and desalted using a Microcon-100 spin column (Millipore). cDNA synthesis was performed on the eluate with the iScript cDNA synthesis kit (Bio-Rad). All manipulations were conducted according to the manufacturer's instructions. First strand cDNA was diluted to a final concentration of 5 ng/µl (total RNA equivalent). RT-PCR amplification reactions were carried out in a total volume of 7.5 µl, containing 10 ng of template cDNA, 3.75 µl of 2x SYBR Green I reaction mix (Eurogentec), 1 µl nuclease-free water (Sigma) and 0.375 µl of a 5 µM solution of each primer. Cycling conditions were as follows: 10 min at 95°C followed by 45 cycles of denaturation (10s at 95°C) and elongation (45s at 60°C). All reactions were performed on a LightCycler 480 (Roche). Primers were designed using Primer3 (Rozen and Skaletsky, 2000) and validated through RTPimerDB's in silico assay evaluation pipeline (Lefever et al., 2009). Raw Cq values were imported into qbaseplus (Hellemans et al., 2007) (www.biogazelle.com) and normalized using a selection of stably expressed reference genes (UBC, SDHA, GAPDH and Alu-sx). Primer sequences for UBC, SDHA and GAPDH are available in the public RTprimerDB database (http://www.rtprimerdb.org/) (gene (RTPrimerDB-ID): UBC(8), SDHA(7), GAPDH(3)). For Alu-sx, the following primer sequences were used: F: TGGTGAAACCCCGTCTCTACTAA, R: CCTCAGCCTCCCGAGTAGCT.

miRNA expression profiling and data normalization were performed as described previously (Mestdagh et al., 2008; Mestdagh et al., 2009b).

Pre-miR transfection

Individual pre-miR molecules (Ambion) were transfected in neuroblastoma SHEP-cells at a concentration of 100 nM using Xtremegene transfection reagent (Roche) according to the manufacturer's instructions. Pre-miR negative control #1 (Ambion) was used as a scrambled control. Transfection efficiency was monitored by flow cytometry using a fluorescently labeled pre-miR (Ambion) and estimated to be 80% or higher. Cells were cultured in RPMI

(Invitrogen), 10% FCS in the absence of antibiotics. Cells were harvested for RNA isolation (miRNeasy, Qiagen) 24h post transfection.

3'UTR luciferase constructs

3'UTR luciferase reporter constructs for TGFBR2 were obtained from Switchgear Genomics. For SMAD2 and SMAD4, 74 bp oligonucleotides spanning the predicted 3'UTR miRNA binding site and flanked by XhoI and NotI restriction sites were cloned into psicheck2 (Promega) as described previously (Cloonan et al., 2008). The following oligonucleotides were used:

SMAD2_miR-18a_F

TCGAGAAAACAGCACTTGAGGTCTCATCAATTAAA**GCACCTT**GTGGAATCTGTTTCCTATATTTGAATATTAGC

SMAD2_miR-18a_R

GGCCGCTAATATTCAAATATAGGAAACAGATTCCACAAGGTGCTTTAATTGATGAGACCTCAAGTGCTGTTTTC

SMAD2_miR-19_F

TCGAGCCTTCCTCAACCTTTGCTGTAAAAATTTCA**TTTGCAC**CACATCAGTACTACTTAATTTAACAAGCTTGC

SMAD2_miR-19_R

GGCCGCAAGCTTGTTAAATTAAGTAGTACTGATGTGGTGCAAATGAAATTTTTACAGCAAAGGTTGAGGAAGGC

SMAD2_miR-92a_F

TCGAGTTTTTTTCTCTGATGGCATTAACTTTGTAA**TGCAATA**TGATGGATGCAGACCCTGTTCTTGTTTCCCGC

SMAD2_miR-92a_R

GGCCGCGGGAAACAAGAACAGGGTCTGCATCCATCATATTGCATTACAAAGTTAATGCCATCAGAGAAAAAAAC

SMAD4_miR-18a_F

TCGAGAAGACTTAATTTTAACCAAAGGCCTAGCAC**CACCTTA**GGGGCTGCAATAAACACTTAACGCGCGCACGC

SMAD4_miR-18a_R

GGCCGCGTGCGCGCGTTAAGTGTTTATTGCAGCCCCTAAGGTGGTGCTAGGCCTT
TGGTTAAAATTAAGTCTTC

SMAD4_ miR-19_miR-17/20_ F

TCGAGGTTTGATTTTTAAGATTTTTTTTTTCT**TTTGCACTTT**TGAGTCCAATCTCA
GTGATGAGGTACCTTCGC

SMAD4_ miR-19_miR-17/20_ R

GGCCGCGAAGGTACCTCATCACTGAGATTGGACTCAAAAGTGCAAAAGAAAAAA
AAAATCTTAAAAATCAAACC

SMAD2_miR-18a_mut_F

TCGAGAAAACAGCACTTGAGGTCTCATCAATTAAA**TCCAATT**GTGGAATCTGTTT
CCTATATTTGAATATTAGC

SMAD2_miR-18a_mut_R

GGCCGCTAATATTCAAATATAGGAAACAGATTCCACAATTGGATTTAATTGATGA
GACCTCAAGTGCTGTTTTC

SMAD4_miR-18a_mut_F

TCGAGAAGACTTAATTTTAACCAAAGGCCTAGCAC**TACTTTC**GGGGCTGCAATA
AACACTTAACGCGCGCACGC

SMAD4_miR-18a_mut_R

GGCCGCGTGCGCGCGTTAAGTGTTTATTGCAGCCCCGAAAGTAGTGCTAGGCCTT
TGGTTAAAATTAAGTCTTC

For TGFBR2, miRNA binding sites were mutated using the Quickchange site-directed mutagenesis kit (Agilent) according to the manufacturer's instructions. The following primers were used:

TGFBR2_miR-17/20_1_F

GATTGATTTTTACAATAGCCAATAACATTTTCCAGTTATTAATGCCTGTATATAAA
TATGAATAGCTA

TGFBR2_miR-17/20_1_R

TAGCTATTCATATTTATATACAGGCATTAATAACTGGAAAATGTTATTGGCTATTG
TAAAAATCAATC

TGFBR2_miR-17/20_2_F

GGTCAGCACAGCGTTTCAAAAAGTGAAGCAAAGGTATAAATATTTGGAGATTTTG
CAGGAAAA

TGFBR2_miR-17/20_2_R

TTTTCCTGCAAAATCTCCAAATATTTATACCTTTGCTTCACTTTTTGAAACGCTGTG
CTGACC

miRNA target site analysis

Four miRNA seed types were considered for miRNA target site analyses: 6mer, 7mer-A1, 7mer-m8 and 8mer sites (Grimson et al., 2007). Target sites were identified using a custom Perl script. 5' UTR, CDS and 3'UTR sequences were taken from Baek et al. (Baek et al., 2008).

Candidate miR-17-92 target gene selection

Genes with a protein expression fold change below -0.5 (log2) and at least one 3' UTR miR-17-92 site were selected as candidate miR-17-92 target genes. The expression fold change cutoff of 0.5 was selected as the fold change that deviated from the linear fit in a normal QQ-plot. Throughout the manuscript, downregulated proteins are defined by a log2 expression fold change < -0.5, upregulated proteins by a log2 expression fold change > 0.5.

Xenografts

SHEP-TR-miR-17-92 and SHEP-TR (control) cells were transfected with a luciferase expressing mammalian vector. This vector was obtained by cloning the firefly luciferase gene under the control of a CMV promoter and enables bioluminescent imaging of viable cells in vivo. Stable clones obtained after 15 days of selection in 300ug/ml hygromicine (Sigma, USA) were evaluated for their bioluminescence signal by serial cellular dilutions incubated with the luciferine substrate. The bioluminescence signal was acquired by an IVIS illumina 3D Imaging System (Xenogen Corp. Alameda, CA). Etherotopic xenografts were established in atymic nude mice (n=5) by injection of 106 SHEP-TR cells subcutaneosly in the left flanking site and 106 SHEP-TR-miR-17-92 cells in the rigth flanking site of each individual animal. Mice were fed with tetracycline (from SIGMA) once a day using oral gavage prestige 200ul (2mg/ml in ddH2O). In vivo tumorigenic bioluminiscence imaging was performed by

measuring bioluminescence (BLI, phothon/sec) of luciferine positive living cells at 0, 7, 14 and 21 days post injection, measuring the median value of emissions from three scans per animal at each flanking site.

Immunohistochemistry and Western blot

SHEP-TR-miR-17-92 cells, tetracycline treated or untreated, were stimulated with TGFβ1 for 4 h. After harvesting, 200 µl of cell suspension were centrifuged on a cytospin glass using a cytospin chamber. The cytopreparations were air dried, fixed with 4% paraformaldehyde (Sigma Aldrich, Munich, Germany) for 10 min followed by 45 min in Tris-1% Triton buffer. After antigen retrieval, pSMAD2 immunoreactivity (anti-pSMAD2, Cell Signaling) was detected using the Dako Auto-stainer Plus (Glostrup, Denmark) and the Dako EnVision Flex system (Glostrup, Denmark) according to the manufacturer´s instructions. For Western blot analysis, cells were lysed in RIPA buffer, separated on a SDS–PAGE gel and blotted onto Immobilon-P (Millipore, Bedford, MA, USA) membrane. The membrane was incubated with anti-phosphorylated SMAD2 (pSMAD2, Cell Signaling Technology) or anti-ACTIN (ICN Biomedicals, Aurora, OH, USA). HRP-conjugated secondary antibodies were obtained from Amersham Biosciences. Proteins were detected by Super Signal chemiluminescence substrate (Pierce, Rockford, IL, USA). Images were processed using ImageJ software.

Statistics

All statistical analyses were performed using R Bioconductor software. For survival analysis, rank-based pathway scores were calculated as described previously (Fredlund et al., 2008; Mestdagh et al., 2009a). Samples (n) were ranked according to the expression level of each gene/miRNA within the set and rank scores (ranging from 1 to n) were assigned. This was repeated for each gene in the gene set. Next, rank scores were summed generating an activity score of the gene/miRNA set for each sample. Kaplan-Meier analysis was performed using pathway activity score quartiles.

MiRNA target site overrepresentation was evaluated using Fisher's Exact test in combination with Bonferroni multiple testing correction. Differential expression/activity was evaluated using the Mann-Whitney test, unless stated otherwise.

For the identification of relevant biological pathways among the up- and down-regulated proteins, a gene list ranked according to protein expression was analyzed using GSEA with the chemical and genetic perturbations collection (Subramanian et al., 2005). Gene lists with a false discovery rate (FDR) below 5% were considered significant. For calculation of individual miR-17-92 miRNA contributions to the significant gene lists the contributing genes

of each gene list were analyzed for the presence of 7mer and 8mer miR-17-92 sites. For each gene list, the fraction of targets per individual miR-17-92 miRNA was calculated. Data was log transformed and standardized before hierarchical clustering (method: Ward, distance: Manhattan). Gene lists with two or more missing values were excluded for clustering purposes.

Cell adhesion and proliferation assays

To evaluate cell adhesion, ells were quickly washed in Versene and then incubated at 37°C in the presence of Versene. After 15 min, the cells were visualized under a microscope to assure that the cell-cell contacts were disrupted. The cells were then counted, centrifuged and suspended in medium (RPMI, 10% FCS) at a concentration of 2x106 cells/ml and thereafter incubated on a rotating platform at 37°C for 1 h and then analyzed. Each treatment was assayed in triplicate and repeated three times. Pictures were processed using ImageJ software.
For cell proliferation, SHEP-TR-miR-17-92 cells were trypsinized and seeded in 96-well xCELLigence E-plates (Roche) (10000 cells/well) according to the manufacturer's instructions. After 24 h, cells were either treated with tetracycline or left untreated and were monitored in real-time on the xCELLigence system. Five replicate measurements per condition were obtained. SMAD2/SMAD4 overexpression For overexpression of SMAD2 and SMAD4 SHEP-TR-miR-17-92 cells were seeded in 6-well plates 12 hours prior to transfection at a density of 100,000 cells per well. The cells were then transfected with either pFLAG-SMAD2, pFLAG-SMAD4 (400 ng/well, respectively) and pEGFP-C1 (Clontech, USA) vectors (200 ng/well) or control pHA-CMV (Clontech, USA) (800 ng/well) and pEGFP-C1 vectors (200 ng/well) using Lipofectamine transfection reagent in OptiMEM I Reduced Serum Medium. The cells were thereafter grown for 48 hours in RPMI (Invitrogen) supplemented with fetal calf serum (1%) tetracycline containing medium. GFP transfection and total cell count was assessed using the Nucleocounter 3000 system (Chemotek, Denmark).

CAGA-Luciferase reporter assay

For luciferase experiments, tetracycline or control treated SHEP-TR-miR-17-92 cells were seeded in 96-well plates 12 hours prior to transfection at a density of 10000 cells per well. The cells were then transfected with the (CAGA)12-Luc luciferase reporter vector containing twelve CAGA SMAD binding sites (Dennler et al., 1998) (400 ng/well) using Lipofectamine 2000 transfection reagent in OptiMEM I Reduced Serum Medium. Following transfection, cells were treated as indicated in the figure legends. Cells were lysed and assayed for luciferase and renilla activity using the Dual-Luciferase Reporter Assay System (Promega,

Madison, WI, USA) and a TD-20/20 Luminometer (Turner Biosystems, Sunnyvale, CA, USA).

Supplemental References

Baek, D., Villen, J., Shin, C., Camargo, F.D., Gygi, S.P., and Bartel, D.P. (2008). The impact of microRNAs on protein output. Nature 455, 64-71.

Cloonan, N., Brown, M.K., Steptoe, A.L., Wani, S., Chan, W.L., Forrest, A.R., Kolle, G., Gabrielli, B., and Grimmond, S.M. (2008). The miR-17-5p microRNA is a key regulator of the G1/S phase cell cycle transition. Genome Biol 9, R127.

Colaert, N., Helsens, K., Impens, F., Vandekerckhove, J., and Gevaert, K. (2010). Rover: a tool to visualize and validate quantitative proteomics data from different sources. Proteomics 10, 1226-1229.

Dennler, S., Itoh, S., Vivien, D., ten Dijke, P., Huet, S., and Gauthier, J.M. (1998). Direct binding of Smad3 and Smad4 to critical TGF beta-inducible elements in the promoter of human plasminogen activator inhibitor-type 1 gene. EMBO J 17, 3091-3100.

Elias, J.E., and Gygi, S.P. (2007). Target-decoy search strategy for increased confidence in large-scale protein identifications by mass spectrometry. Nat Methods 4, 207-214.

Fredlund, E., Ringner, M., Maris, J.M., and Pahlman, S. (2008). High Myc pathway activity and low stage of neuronal differentiation associate with poor outcome in neuroblastoma. Proc Natl Acad Sci U S A 105, 14094-14099.

Gevaert, K., Van Damme, J., Goethals, M., Thomas, G.R., Hoorelbeke, B., Demol, H., Martens, L., Puype, M., Staes, A., and Vandekerckhove, J. (2002). Chromatographic isolation of methionine-containing peptides for gel-free proteome analysis: identification of more than 800 Escherichia coli proteins. Mol Cell Proteomics 1, 896-903.

Ghesquiere, B., Colaert, N., Helsens, K., Dejager, L., Vanhaute, C., Verleysen, K., Kas, K., Timmerman, E., Goethals, M., Libert, C., et al. (2009). In vitro and in vivo protein-bound tyrosine nitration characterized by diagonal chromatography. Mol Cell Proteomics 8, 2642-2652.

Grimson, A., Farh, K.K., Johnston, W.K., Garrett-Engele, P., Lim, L.P., and Bartel, D.P. (2007). MicroRNA targeting specificity in mammals: determinants beyond seed pairing. Mol Cell 27, 91-105.

Hellemans, J., Mortier, G., De Paepe, A., Speleman, F., and Vandesompele, J. (2007). qBase relative quantification framework and software for management and automated analysis of real-time quantitative PCR data. Genome Biol 8, R19.

Lefever, S., Vandesompele, J., Speleman, F., and Pattyn, F. (2009). RTPrimerDB: the portal for real-time PCR primers and probes. Nucleic Acids Res 37, D942-945.

Mestdagh, P., Feys, T., Bernard, N., Guenther, S., Chen, C., Speleman, F., and Vandesompele, J. (2008). High-throughput stem-loop RT-qPCR miRNA expression profiling using minute amounts of input RNA. Nucleic Acids Res 36, e143.

Mestdagh, P., Fredlund, E., Pattyn, F., Schulte, J.H., Muth, D., Vermeulen, J., Kumps, C., Schlierf, S., De Preter, K., Van Roy, N., et al. (2009a). MYCN/c-MYC-induced microRNAs repress coding gene networks associated with poor outcome in MYCN/c-MYC-activated tumors. Oncogene.

Mestdagh, P., Van Vlierberghe, P., De Weer, A., Muth, D., Westermann, F., Speleman, F., and Vandesompele, J. (2009b). A novel and universal method for microRNA RT-qPCR data normalization. Genome Biol 10, R64.
Oberthuer, A., Berthold, F., Warnat, P., Hero, B., Kahlert, Y., Spitz, R., Ernestus, K., Konig, R., Haas, S., Eils, R., et al. (2006). Customized oligonucleotide microarray gene expression-based classification of neuroblastoma patients outperforms current clinical risk stratification. J Clin Oncol 24, 5070-5078.
Perkins, D.N., Pappin, D.J., Creasy, D.M., and Cottrell, J.S. (1999). Probability-based protein identification by searching sequence databases using mass spectrometry data. Electrophoresis 20, 3551-3567.
Rozen, S., and Skaletsky, H. (2000). Primer3 on the WWW for general users and for biologist programmers. Methods Mol Biol 132, 365-386.
Subramanian, A., Tamayo, P., Mootha, V.K., Mukherjee, S., Ebert, B.L., Gillette, M.A., Paulovich, A., Pomeroy, S.L., Golub, T.R., Lander, E.S., and Mesirov, J.P. (2005). Gene set enrichment analysis: a knowledge-based approach for interpreting genome-wide expression profiles. Proc Natl Acad Sci U S A 102, 15545-15550.